

# Reactions of Olefins with Ruthenium Hydride Nanoparticles: NMR Characterization, Hydride Titration, and Room-Temperature C–C Bond Activation\*\*

Jordi García-Antón, M. Rosa Axet, Susanna Jansat, Karine Philippot, Bruno Chaudret,\* Tal Pery, Gerd Buntkowsky, and Hans-Heinrich Limbach

Metal nanoparticles have been used for a long time to catalyze chemical reactions in both heterogeneous and homogeneous phases.<sup>[1]</sup> The analysis of traditional heterogeneous and homogeneous catalysis requires very different techniques that are difficult to combine for the study of metal nanoparticles, in which distinguishing between colloidal and molecular catalysis is difficult.<sup>[2]</sup> Thus, many questions concerning the reactivity of metal nanoparticles are still open, particularly the nature of intermediate surface species, knowledge of which is important for the development of new nanocatalysts and new catalytic transformations. Some of us have used solid-state NMR spectroscopy for this purpose recently,<sup>[3]</sup> and herein we report the combination of this method with desorption techniques for investigating the reactivity of ruthenium nanoparticles.

The synthesis of metal nanoparticles by hydrogenation of organometallic precursors in the presence of organic ancillary ligands, such as amines, thiols, or carboxylic acids as stabilizers, has been investigated for over fifteen years by some of us.<sup>[4]</sup> In particular, essentially monodisperse, very small ruthenium nanoparticles, which display a remarkable surface coordination chemistry, can be obtained using [Ru(cod)(cot)] as a precursor (cod = 1,5-cyclooctadiene; cot = 1,3,5-cyclooctatriene). This system, and similar ones involving Pd, Pt, or Rh nanoparticles, catalyzes a number of chemical reactions such as olefin hydrogenation, C–C coupling, and

hydrogenation of aromatic hydrocarbons.<sup>[5]</sup> Some of us have shown independently that palladium nanoparticles stabilized by asymmetric phosphite groups are good enantioselective alkylation catalysts.<sup>[6]</sup> This result provides strong evidence for the direct coordination of ligands, in this case phosphite groups, to the palladium surface.

The coordination of ligands such as CO,<sup>[7]</sup> amines,<sup>[8]</sup> and organosilanes,<sup>[9]</sup> has previously been established by NMR spectroscopy studies in solution or in the solid state. The coordination of hydrogen to metal nanoparticles, however, is especially important. Hydrogen binding to clean metal surfaces has been well established by surface science, and it is generally accepted that one hydrogen atom is adsorbed per surface metal atom.<sup>[10]</sup> We have recently demonstrated the presence of mobile hydrides, which are in slow exchange with gaseous dihydrogen, on the surface of amine-protected ruthenium nanoparticles using a combination of gas-phase <sup>1</sup>H NMR and solid-state <sup>2</sup>H NMR spectroscopy.<sup>[3]</sup> Furthermore, other species, such as alkenes or arenes, may adsorb on the surface during a catalytic process or give rise to new reactive intermediates, including alkyl groups and carbenes. The important question which then arises is whether these groups are stable and can be detected spectroscopically, as in organometallic complexes.

Herein we describe: 1) the synthesis of a new class of phosphine-protected ruthenium nanoparticles, 2) the characterization of phosphine coordination by NMR spectroscopy techniques, 3) the presence and the quantification of hydrides on the surface of ruthenium nanoparticles stabilized by a polymer (polyvinylpyrrolidone, PVP), diphosphines (1,4-bis(diphenylphosphino)butane (dppb) and 1,10-bis(diphenylphosphino)decane (dppd)), or amines (hexadecylamine (HDA)), and 4) our exploration of the reactivity of these nanoparticles by NMR spectroscopy, which has led to the discovery of a novel reaction.

The ruthenium nanoparticles were prepared as described previously by hydrogenation of the organometallic precursor [Ru(cod)(cot)] in THF at room temperature. Nanoparticles stabilized by the diphosphines dppb and dppd were synthesized in the same way by adding 0.1 molar equivalents of diphosphine per ruthenium. The nanoparticles were precipitated by addition of pentane and redissolved in THF for solution NMR spectroscopy studies. They were found to have a mean size of 1.5 ± 0.3 (dppb) and 1.9 ± 0.5 nm (dppd; Figure 1), and the hexagonal close packed (hcp) structure of bulk ruthenium was demonstrated by wide-angle X-ray scattering (WAXS) studies.

[\*] Dr. J. García-Antón, Dr. M. R. Axet, Dr. S. Jansat, Dr. K. Philippot, Dr. B. Chaudret  
Laboratoire de Chimie de Coordination du CNRS  
205, route de Narbonne, 31077 Toulouse Cedex 04 (France)  
Fax: (+33) 5-6155-3003  
E-mail: chaudret@lcc-toulouse.fr

T. Pery, Prof. H.-H. Limbach  
Institut für Chemie, Freie Universität Berlin  
Takustrasse 3, 14195 Berlin (Germany)

Prof. G. Buntkowsky  
Institut für Physikalische Chemie  
FSU Jena, Helmholtzweg 4, 07743 Jena (Germany)

[\*\*] The authors thank V. Collière and L. Datas (UPS-TEMSCAN) for TEM/HRTEM measurements, P. Lecante (CEMES-CNRS) for WAXS analysis, J. F. Meunier (LCC-CNRS) for MS analyses, and S. Maynadié-Parres (LCC-CNRS) for recording the MAS NMR spectra. We are grateful to the CNRS for financial support, in particular for the CNRS-DFG bilateral project no. 1372. J.G.-A. thanks the Ministerio de Educación y Ciencia de España for a postdoctoral fellowship (EX2004-0039).

Supporting information for this article is available on the WWW under <http://www.angewandte.org> or from the author.

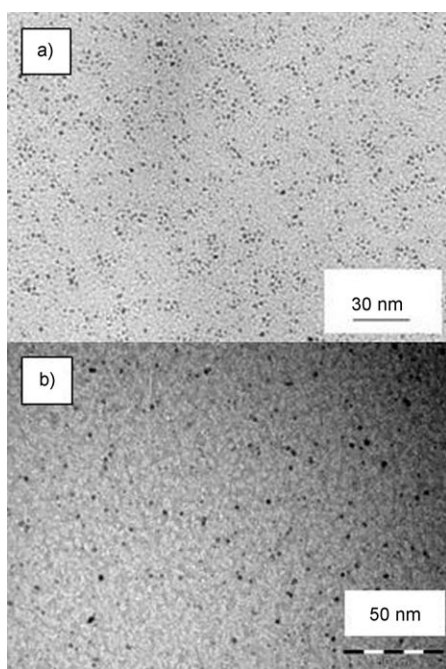


**Figure 1.** TEM images of Ru nanoparticles stabilized by dppb (a) and dppd (b).

Coordination of the phosphine groups was investigated by NMR spectroscopy. No signal is visible in the  $^{31}\text{P}$  NMR spectrum of Ru/dppb nanoparticles recorded in  $[\text{D}_8]\text{THF}$  solution. However, addition of a few drops of  $\text{H}_2\text{O}_2$  leads to the immediate appearance of new peaks at around  $\delta = 4, 33,$  and  $58$  ppm, which were attributed to an unoxidized diphenylphosphino moiety and to phenyl and alkyl phosphine oxide moieties, respectively (see the Supporting Information). This experiment demonstrates both the coordination of the phosphine groups to the nanoparticles and their release after oxidation, and the absence of both free phosphine and exchange processes on the NMR timescale in the initial solution. In addition, it also demonstrates the hydrogenation of some phenyl groups during the synthesis process.

The absence of solution NMR signals from the nuclei coordinated to a nanoparticle has been observed and discussed previously and may be due to several factors, including a Knight shift, fast  $T_2$  relaxation resulting from the slow tumbling of the particles in solution, and surface anisotropy.<sup>[11]</sup> To distinguish between these factors, the nanoparticles were characterized by cross-polarization magic-angle spinning (CP-MAS) solid-state NMR spectroscopy. The  $^{13}\text{C}$  MAS NMR spectra of Ru/dppb and Ru/dppd exhibit peaks at  $\delta = 26$  ppm corresponding to alkyl carbon atoms and at  $\delta = 130$  ppm corresponding to aromatic carbons for Ru/dppb and only signals characteristic of alkyl carbon atoms near  $\delta = 30$  ppm for Ru/dppd. Similarly, the  $^{31}\text{P}$  MAS NMR spectrum of Ru/dppb shows two broad signals near  $\delta = 50$  and  $25$  ppm, while that of Ru/dppd exhibits an intense broad signal at  $\delta = 55$  ppm with a shoulder near  $\delta = 30$  ppm (see the Supporting Information), in agreement with the coordination of dialkyl- and diphenylphosphino groups, respectively, at the surface of the particles. This study shows that 1) the absence

of a signal in solution is not due to a magnetic effect, and 2) the lack of surface homogeneity causes an important broadening of the signals but does not prevent them being observed. The absence of a signal in solution is therefore clearly due to a relaxation problem, as previously observed for the alkyl chains of thiol-stabilized gold nanoparticles by  $^{13}\text{C}$  NMR spectroscopy.<sup>[11]</sup>

As mentioned above, we have previously detected the presence of hydrides on the surface of Ru nanoparticles stabilized by HDA by a combination of NMR spectroscopic methods.<sup>[3]</sup> We have also been able to detect mobile hydrogens on ruthenium nanoparticles stabilized by PVP or by diphosphine ligands using the same methods.<sup>[12]</sup> However, we were only able to obtain a qualitative indication about the adsorption of hydrogen onto the Ru nanoparticles' surface, whereas quantitative information is required to shed some light on the actual surface coverage of the Ru nanoparticles. Since ruthenium nanoparticles are very active hydrogenation catalysts, we decided to titrate the surface hydrides with olefins and measure the amount of alkane formed by GC analysis. Two olefins with different structures, namely 1-octene and norbornene, at two different concentrations (1 and 5 equivalents with respect to the total amount of Ru present in the particles) were used to eliminate artifacts. Three different nanoparticle systems were tested, namely Ru/HDA, which has previously been shown to contain hydrides,<sup>[3]</sup> Ru/PVP, and Ru/dppd, which, respectively, contain particles in a polymer that displays limited interactions and particles firmly attached to phosphine ligands. Remarkably, we found that for a given nanoparticle system, and within the limits of experimental error, the same conversion was reached with either one or five equivalents of either 1-octene or norbornene (Table 1). This result suggests that a definite and

**Table 1:** Conversion of olefins into alkanes with the different Ru nanoparticles systems.

Olefin	Nanoparticle system	[olefin]/initial [Ru] ratio					
		1:1		5:1		1:1	
		2 h	18 h	24 h	24 h	24 h	24 h
1-Octene	Ru/PVP	0.47	0.49	0.50	0.50	0.51	0.49
	Ru/HDA	0.29	0.29	0.34	0.34	0.33	0.35
	Ru/dppd	0.24	0.31	0.26	0.32	0.27	0.31
Norbornene	Ru/PVP	0.44	0.42	0.49	0.47	0.50	0.48
	Ru/HDA	0.26	0.32	0.30	0.32	0.30	0.32
	Ru/dppd	0.21	0.32	0.26	0.30	0.26	0.31

reproducible number of hydrides are present at the nanoparticles' surface. The kinetics of the reaction follow the trend  $\text{Ru/PVP} > \text{Ru/HDA} > \text{Ru/dppd}$ , and these results are in agreement with the steric hindrance present at the surface of the particles. The Ru/PVP and Ru/dppd nanoparticles display a very narrow size distribution. If we assume that the particles are monodisperse and perfectly spherical, given their mean size of 1.5 and 1.9 nm, respectively, and their structure (hcp), the calculated percentage of ruthenium atoms at their surface is 76% and 52%, respectively. The Ru/HDA particles are slightly elongated, but in a first approximation they can be

considered as spheres with a mean diameter of 1.9 nm and therefore to also contain 52% of their ruthenium atoms at their surface. Knowing the total amount of ruthenium introduced and the conversion of the olefins, it is then easy to calculate the number of hydrides consumed in the hydrogenation process (approximately 1.3, 1.3, and 1.1 hydrides per surface ruthenium atom for the Ru/PVP, Ru/HDA, and Ru/dppd nanoparticles respectively).

We performed the following experiments to determine the fate of the ruthenium nanoparticles (“Ru”) after the hydrogenation process and the nature of the species adsorbed on their surfaces spectroscopically. Following a method similar to that described previously for the Vaska complex,<sup>[13]</sup> we allowed gaseous ethylene to react with solid Ru/dppb nanoparticles in an NMR tube closed with a Teflon needle valve in the absence of solvent and observed the presence of both gaseous ethylene and ethane by gas-phase <sup>1</sup>H NMR spectroscopy. When we performed the reaction with tetradeuterioethylene, we observed a mixture of [D<sub>1</sub>]/[D<sub>3</sub>]ethylene and [D<sub>1</sub>]/[D<sub>3</sub>]ethane. The resulting ruthenium nanoparticles were studied by solid-state <sup>2</sup>H NMR spectroscopy under the condition of slow magic-angle spinning (3.0 kHz). Figure 2a

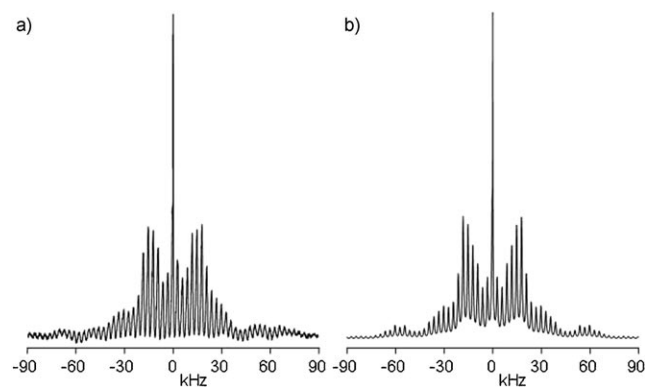


**Figure 2.** a) <sup>2</sup>H NMR MAS spectrum of Ru/dppb nanoparticles after reaction with D<sub>2</sub>C=CD<sub>2</sub>; b) SIMPSON simulation of the spectrum employing a mobile CD<sub>3</sub> group ( $q_{cc} = 55$  kHz), an immobile CD group ( $q_{cc} = 173$  kHz), and two liquid-like Lorentzian lines in the center.

depicts a spectrum obtained at room temperature, a simulation with the SIMPSON program is shown in Figure 2b.<sup>[14]</sup> The envelope of the spinning side-band pattern indicates the presence of three spectral components. The major component is a relatively narrow side-band spectrum with a quadrupole coupling constant,  $q_{cc}$ , of 50–55 kHz. This value is characteristic of the presence of methyl groups undergoing fast, threefold 120° jumps, which reduce the intrinsic  $q_{cc}$  of 167 kHz to the observed value.<sup>[15]</sup> The rotation axis itself may be subject to a slow rotational diffusion or “reorientation” on the second to millisecond timescale. We assign this spectral component to surface methyl groups bound to the nanoparticles. The second broad component, which exhibits a lower intensity, is characterized by a large quadrupole coupling constant of 160–170 kHz. We assign this component to immobilized CD groups in PVP, which are formed by H/D exchange with surface deuterons prior to the reaction with

ethylene, as described previously for other ligands.<sup>[3]</sup> Finally, the sharp component in the center of the signal indicates the presence of rapidly reorientating deuterons, which could be either mobile surface deuterons<sup>[3]</sup> or mobile deuterated ethane in the particles.

To corroborate the presence of the postulated surface methyl groups by solid-state <sup>13</sup>C NMR spectroscopy we allowed Ru/PVP and Ru/dppd particles to react with gaseous <sup>13</sup>CH<sub>2</sub>=<sup>13</sup>CH<sub>2</sub>. Figures 3a and b show the proton-decoupled

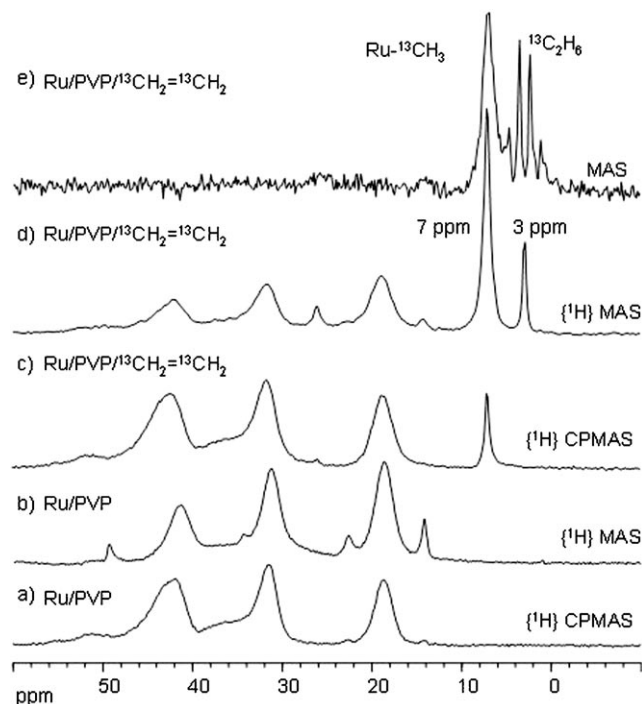


**Figure 3.** Room-temperature solid-state <sup>13</sup>C NMR spectra of Ru/PVP samples in the absence and presence of <sup>13</sup>CH<sub>2</sub>=<sup>13</sup>CH<sub>2</sub> obtained under various experimental conditions. See text for details.

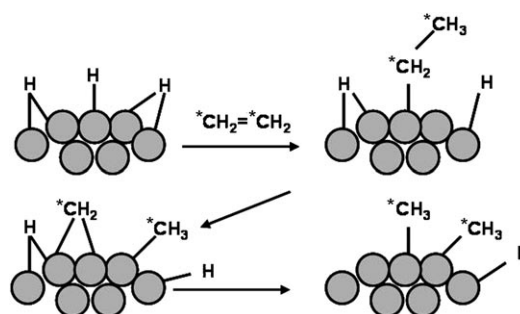
MAS spectra of Ru/PVP obtained with and without <sup>1</sup>H–<sup>13</sup>C cross-polarization (CP). These spectra only show signals arising from PVP and were not analyzed further. With CP only rigid carbon centers exhibiting long longitudinal relaxation times ( $T_1$ ) are detected, whereas without CP only mobile carbon center with shorter  $T_1$  are detected. Addition of gaseous <sup>13</sup>CH<sub>2</sub>=<sup>13</sup>CH<sub>2</sub> results in a new signal at  $\delta = 7$  ppm when using CP (Figure 3c), which grows substantially without CP (Figure 3d). The latter spectrum also contains a sharp peak at  $\delta = 3$  ppm. The chemical shifts of both these new peaks are typical for methyl groups. To characterize the two peaks further we recorded a spectrum without CP and without <sup>1</sup>H decoupling (Figure 3e). The peak at  $\delta = 3$  ppm is now split into a quadruplet with a  $J_{C,H}$  coupling constant of about 120 Hz, whereas the peak at  $\delta = 7$  ppm is broadened slightly. We assigned the peak at  $\delta = 3$  ppm to “liquid”-type methyl groups, which undergo fast 120° jumps and rapid rotational diffusion. Such a methyl group would contribute to the sharp central line in the <sup>2</sup>H NMR spectra of Figure 2 along with the mobile surface deuterons. In contrast, we assigned

the peak at  $\delta = 7$  ppm to “solid”-type methyl groups, which give rise to the dominant side-band pattern in the  $^2\text{H}$  NMR spectra in Figure 2. As the dipolar C–H coupling is reduced by the  $120^\circ$  jumps and the  $^{13}\text{C}$  chemical shift anisotropy of methyl groups is only about  $\delta = 20$  ppm,<sup>[16]</sup> both interactions are almost completely averaged out by MAS. In other words, we can assign the signal at  $\delta = 7$  ppm to surface methyl groups bound to Ru. Interestingly, the signal at  $\delta = 7$  ppm is broad but sharper than would be expected for the envelope of a quartet arising from  $J$  coupling with the methyl protons, although such a coupling would normally be expected. The lack of such a coupling can be explained in terms of  $^1\text{H}$ – $^1\text{H}$  spin diffusion of immobilized methyl groups, which leads to self-decoupling.<sup>[17]</sup> Thus, a substantial part of the linewidth of the signal at  $\delta = 7$  ppm arises from the coalescence of the  $J$ -coupling pattern. We also note that the C–H coupling constant of a methyl group can also be somewhat reduced by agostic interactions.<sup>[18]</sup>

We carried out desorption experiments on the Ru/PVP system, which is least likely to generate artifacts, to try and identify the nature of these methyl-containing surface species. However, we only observed a desorption at  $180^\circ\text{C}$  in vacuo. Gas-phase  $^{13}\text{C}$  NMR spectroscopy allowed the detection of a species with a resonance at  $\delta = -9.9$  ppm, which correlates with a broad singlet at  $\delta = 1.6$  ppm in the  $^1\text{H}$  NMR spectrum and clearly corresponds to methane (see the Supporting Information).<sup>[19]</sup> Other signals for  $\text{C}_2$  and higher hydrocarbons were also observed. We also analyzed the gas mixture by mass spectrometry. Comparison with a blank experiment carried out with the same nanoparticles but not treated with ethylene or  $^{13}\text{C}$ -ethylene showed the predominant presence of methane ( $m/z$  16 and 17 when using labeled ethylene) and ethane ( $m/z$  30 and 32) as well as traces of higher hydrocarbons (see the Supporting Information).

The most likely hypothesis to explain the presence of methyl groups at the surface of the ruthenium particles involves the isomerization of ethylene into surface vinylidene fragments of the type  $\text{Ru}=\text{C}=\text{CH}_2$ .<sup>[20]</sup> However, no signal was observed around  $\delta = 45$  ppm for the methyl group in this fragment.<sup>[21]</sup> Furthermore, we were not able to find the corresponding signal of the carbon bound to Ru when using a fully  $^{13}\text{C}$ -enriched substrate, whereas a phosphine group linked to the surface is detected by  $^{31}\text{P}$  NMR MAS spectroscopy (see the Supporting Information). Likewise, the chemical shift of the methyl groups and the desorption experiments unambiguously show the presence of methane and ethane, which agrees with the presence of methyl groups on the ruthenium surface. This implies the activation of a C–C bond under very mild conditions in all three types of nanoparticles studied (Ru/PVP, Ru/HDA, and Ru/dppd). The mechanism of this reaction is still unknown but a reasonable pathway would involve insertion of ethylene into a remaining surface hydride to give a surface ethyl species, followed by  $\beta$ -alkyl transfer to the surface, as illustrated in Scheme 1. The subsequent step could involve rehydrogenation of the surface methylene moiety by the remaining surface hydrogens.

The characterization of surface methyl groups after a hydrogenation process has been reported previously in a work on the deactivation of an industrial heterogeneous palladium-



**Scheme 1.** Reaction of ethylene with hydrides at the surface of Ru nanoparticles.

based hydrogenation catalyst and correlates well with our observation of the stability of these surface-bound methyl groups.<sup>[22]</sup>

In summary, we have reported the characterization of phosphine coordination by NMR spectroscopy and the presence and stability of hydrides on the surface of different types of Ru nanoparticles. In all cases we found a hydride/surface Ru ratio greater than 1. In addition, we have clearly demonstrated the presence of surface methyl groups by using a combination of NMR and desorption methods. These groups arise from a carbon–carbon bond cleavage at room temperature, which may turn out to be an important reaction during hydrogenation processes. The reactivity of these methyl groups is currently being explored.

Received: October 15, 2007

Published online: February 5, 2008

**Keywords:** C–C activation · hydride ligands · nanoparticles · ruthenium · surface chemistry

- [1] a) A. Roucoux, J. Schulz, H. Patin, *Chem. Rev.* **2002**, *102*, 3757–3778; b) A. Roucoux, K. Philippot in *Hydrogenation with Noble Metal Nanoparticles in Handbook of Homogenous Hydrogenations* (Ed.: G. de Vries), Wiley-VCH, Weinheim, **2007**, pp. 217–256; c) M. T. Reetz, R. Breinbauer, K. Wanninger, *Tetrahedron Lett.* **1996**, *37*, 4499–4502; d) M. T. Reetz, E. Westermann, *Angew. Chem.* **2000**, *112*, 170–173; *Angew. Chem. Int. Ed.* **2000**, *39*, 165–168; e) M. Moreno-Mañas, R. Pleixats, S. Villarroya, *Organometallics* **2001**, *20*, 4524–4528; f) C. Rocaboy, J. A. Gladysz, *Org. Lett.* **2002**, *4*, 1993–1996; g) C. C. Cassol, A. P. Umptierre, G. Machado, S. I. Wolke, J. Dupont, *J. Am. Chem. Soc.* **2005**, *127*, 3298–3299; h) D. Astruc, F. Lu, J. R. Aranzas, *Angew. Chem.* **2005**, *117*, 8062–8083; *Angew. Chem. Int. Ed.* **2005**, *44*, 7852–7872; i) J. G. de Vries, *Dalton Trans.* **2006**, 421–429.
- [2] a) I. W. Davies, L. Matty, D. L. Hughes, P. Reider, *J. Am. Chem. Soc.* **2001**, *123*, 10139–10140; b) J. A. Widegren, R. G. Finke, *J. Mol. Catal. A* **2003**, *191*, 187–207; c) C. M. Hagen, L. Vieille-Petit, G. Laurency, G. Süß-Fink, R. G. Finke, *Organometallics* **2005**, *24*, 1819–1831; d) L. Vieille-Petit, G. Süß-Fink, B. Therrien, T. R. Ward, H. Stoeckli-Evans, G. Labat, L. Karmazin-Brelot, A. Neels, T. Bürgi, R. G. Finke, C. M. Hagen, *Organometallics* **2005**, *24*, 6104–6119.
- [3] T. Pery, K. Pelzer, G. Buntkowski, K. Philippot, H.-H. Limbach, B. Chaudret, *ChemPhysChem* **2005**, *6*, 605–607.

- [4] a) K. Philippot, B. Chaudret, *C. R. Chim.* **2003**, *6*, 1019–1034; b) B. Chaudret, *Top. Organomet. Chem.* **2005**, *16*, 233–259.
- [5] a) A. Roucoux, *Top. Organomet. Chem.* **2005**, *16*, 261–279; b) S. Jansat, D. Picurelli, K. Pelzer, K. Philippot, M. Gómez, G. Muller, P. Lecante, B. Chaudret, *New J. Chem.* **2006**, *30*, 115–122.
- [6] S. Jansat, M. Gómez, K. Philippot, G. Muller, E. Guiu, C. Claver, S. Castellón, B. Chaudret, *J. Am. Chem. Soc.* **2004**, *126*, 1592–1593.
- [7] J. S. Bradley, J. Millar, E. W. Hill, S. Behal, B. Chaudret, A. Duteil, *Faraday Discuss.* **1991**, *92*, 255–268.
- [8] a) C. Pan, K. Pelzer, K. Philippot, B. Chaudret, F. Dassenoy, P. Lecante, M.-J. Casanove, *J. Am. Chem. Soc.* **2001**, *123*, 7584–7593; b) E. Ramirez, S. Jansat, K. Philippot, P. Lecante, M. Gómez, A. M. Masdeu-Bultó, B. Chaudret, *J. Organomet. Chem.* **2004**, *689*, 4601–4610.
- [9] K. Pelzer, B. Laleu, F. Lefebvre, K. Philippot, B. Chaudret, J.-P. Candy, J. M. Basset, *Chem. Mater.* **2004**, *16*, 4937–4941.
- [10] The interaction of hydrogen with metal single-crystal surfaces has been extensively studied in surface science: a) G. Lauth, E. Schwarz, K. Christmann, *J. Chem. Phys.* **1989**, *91*, 3729–3743; b) R. Döll, L. Hammer, K. Heinz, K. Bedürftig, U. Muschiol, K. Christmann, A. P. Seitsonen, H. Bludau, H. Over, *J. Chem. Phys.* **1998**, *108*, 8671–8679; c) “Hydrogen Transfer on Metal Surfaces”: K. Christmann in *Hydrogen Transfer, Vol. 1* (Eds.: J. T. Hynes, J. P. Klinman, H. H. Limbach and R. L. Schowen), Wiley-VCH, Weinheim, Germany, **2007**, chap. 25, pp. 751–786; for ruthenium, see: d) P. Feulner, D. Menzel, *Surf. Sci.* **1985**, *154*, 465–488; e) M. Y. Chou, J. R. Chelikowsky, *Phys. Rev. Lett.* **1987**, *59*, 1737–1740; f) P. J. Feibelman, J. E. Houston, H. L. Davis, D. G. O’Neill, *Surf. Sci.* **1994**, *302*, 81–92.
- [11] a) R. H. Terrill, T. A. Postlethwaite, C.-H. Chen, C.-D. Poon, A. Terzis, A. Chen, J. E. Hutchison, M. R. Clark, G. Wignall, J. D. Londono, R. Superfine, M. Falvo, C. S. Johnson, Jr., E. T. Samulski, R. W. Murray, *J. Am. Chem. Soc.* **1995**, *117*, 12537–12548; b) A. Badia, W. Gao, S. Singh, L. Demers, L. Cuccia, L. Reven, *Langmuir* **1996**, *12*, 1262–1269.
- [12] B. Wasalek, T. Perry, G. Buntkowsky, H. H. Limbach, J. García-Antón, K. Philippot, B. Chaudret, unpublished results.
- [13] J. Matthes, T. Pery, S. Gründemann, G. Buntkowsky, S. Sabo-Etienne, B. Chaudret, H. H. Limbach, *J. Am. Chem. Soc.* **2004**, *126*, 8366–8367.
- [14] M. Bak, J. T. Rasmussen, N. C. Nielsen, *J. Magn. Reson.* **2000**, *147*, 296–330.
- [15] A. Mittermaier, E. Lewis, L. Kay, *J. Am. Chem. Soc.* **1999**, *121*, 10608–10613.
- [16] V. Tugarinov, C. Scheurer, R. Brüschweiler, L. Kay, *J. Biomol. NMR* **2004**, *30*, 397–406.
- [17] M. Ernst, A. Verhoeven, B. H. Meier, *J. Magn. Reson.* **1998**, *130*, 176–185.
- [18] a) E. Teuma, M. Etienne, B. Donnadiou, G. S. McGrady, *New J. Chem.* **2006**, *30*, 409–415; b) D. G. Maus, V. Copié, B. Sun, J. M. Griffiths, R. G. Griffin, S. Luo, R. R. Schrock, A. H. Liu, S. W. Seidel, W. M. Davis, A. Grohmann, *J. Am. Chem. Soc.* **1996**, *118*, 5665–5671.
- [19] a) L. J. M. van de Ven, J. W. de Haan, *J. Chem. Soc. Chem. Commun.* **1978**, 94–95; b) F. Fleyfel, K. Y. Song, A. Kook, R. Martin, R. Kobayashi, *J. Phys. Chem.* **1993**, *97*, 6722–6725.
- [20] a) R. J. Koestner, M. A. Van Hove, G. A. Somorjai, *Surf. Sci.* **1982**, *121*, 321–337; b) on Ru (0001): C. M. Greenlief, P. L. Radloff, X. L. Zhou, J. M. White, *Surf. Sci.* **1987**, *191*, 93–107.
- [21] See, for example: T. Takao, T. Takemori, M. Moriya, H. Suzuki, *Organometallics* **2002**, *21*, 5190–5203.
- [22] P. Albers, H. Angert, G. Prescher, K. Seibold, S. F. Parker, *Chem. Commun.* **1999**, 1619–1620.